Cascade contribution to the H_2 Lyman band system from electron impact

D. Dziczek, J. M. Ajello, G. K. James, and D. L. Hansen
Jet Propulsion Laboratory, California Institute Of Technology, Pasadena, California 91109
(Received 18 June 1999; published 17 May 2000)

The intensity of UV resonance transitions excited by electron impact is determined by both direct excitation and cascade processes. The lifetime for decay by spontaneous emission from a resonant state is short (typically < 10 ns). Using a pulsed electron gun technique established to separate these two effects we report a laboratory study of the UV spectrum of H_2 attributed to cascade. We utilize the longer lifetimes (> 30 ns) for cascade channels to measure the intense spectrum of the Lyman band system ($B\ ^1\Sigma_u^+ - X\ ^1\Sigma_g^+$) of H_2 populated by cascade from higher lying (EF,GK,H $^1\Sigma_g^+$) states.

PACS number(s): 34.50.Gb, 34.80.Gs

The Lyman ($B\ ^1\Sigma_u^+ - X\ ^1\Sigma_g^+$) band system is the strongest band system of H_2 [1]. The Lyman band system and the remainder of the two Rydberg series of H_2: $^1\Sigma_u^+ 1s\sigma np\sigma(B,B',n=2,3) \rightarrow X\ ^1\Sigma_u^+$ and $^1\Pi_u^+ 1s\sigma np\pi(C,D,n=2,3) \rightarrow X\ ^1\Sigma_u$ are of intense interest to theoreticians [2]. The Lyman band system plays a significant role in astrophysics as a tool for measurement of energy input to astronomical objects such as the Jupiter aurora [3], the outer planets [4], and Herbig-Haro objects in the interstellar medium [5]. In each of these cases collisional excitation of H_2 by electrons results in UV emission from the Rydberg band systems spanning the spectral range 75–170 nm. While giant strides in modeling high resolution laboratory and spacecraft spectra have been made recently (e.g., the transition probability calculations of [2,6]), a complete description of the Lyman band spectrum has proved elusive because of the unknown cascade contributions to the B state of H_2. Specifically the magnitude of the EF,GK,H $^1\Sigma_g^+ \rightarrow B\ ^1\Sigma_u^+$ electron impact cascade contributions to the Lyman band emission spectrum has not been established. The difficulty lies in understanding the optically forbidden excitation to the rovibronic levels of these double-minimum gerade states from the $X\ ^1\Sigma_g^+$ ground state. The present experiment fills this need by providing measurements of the cascade spectrum. Spectral measurements are achieved using a noncontinuous electron beam mode at 20 and 100 eV and gating the photon detector, which eliminates the direct processes based on its short lifetime. Unlike previous approaches (e.g., Mahan, Gallagher, and Smith [7]) this technique enables an entire spectrum rather than an individual transition to be examined in the time domain. The significant result for the Lyman band system is that the cross sections for direct excitation and cascade are nearly equal at 20 eV. The UV spectrum provides a laboratory benchmark spectrum for theoreticians engaged in *ab initio* calculations of electron collision cross sections and transition probabilities for the gerade states of H_2. The mutual coupling interactions of the first five gerade states, including the states of this study, have been described by [8].

The direct and cascade channels contributing to a UV line resonance spectrum can be conveniently separated in the time domain. Lifetimes of the $B\ ^1\Sigma_u^+$ rovibronic levels of H_2 are in the range 0.5–2 ns [2], whereas the lifetimes of the vibronic levels of the EF state are in the range 100–1000 ns [9,10] and the vibronic levels of the GK, H states are in the range 20–100 ns [10,11]. We show in Fig. 1 a schematic of the two principal gerade states that radiatively cascade in the middle ultraviolet (MUV) and visible IR to the $B\ ^1\Sigma_u^+$ rovibronic levels. The low v' levels of the $B\ ^1\Sigma_u^+$ state can be populated by cascade via many rovibronic levels of the GK, H, and EF states. The cumulative effect of these many slow cascades to a rovibronic level can be studied in a pulsed beam experiment by monitoring the intensity of a single fine structure $B \rightarrow X$ line, after the direct excitation has decayed away. This measurement establishes the general experimental methodology for obtaining electron-excited cascade spectra without contamination from direct excitation.

The experimental system in its conventional operating mode of steady-state excitation has been described before [1]. The system consists of a 3 m high-resolution UV spectrometer ($\lambda/\Delta\lambda = 67000$) in tandem with an electron collision chamber. The magnetically collimated electron beam collides at a right angle with a beam of gas effusing from a collimated hole structure. The photon detector is a channel electron multiplier coated with CsI. To operate the electron beam in the pulsed mode the potential of the first accelerating electrode of the gun (L_1) is varied periodically. Figure 2(a) shows the time dependence of the electron impact excitation rate, which is proportional to the instantaneous electron beam current. At the beginning of the pulsing cycle (t_0) the potential of L_1 is changed from a value 20–30 V below the potential of the cathode (which blocks the electron beam) to a value of 2.5 V above the cathode potential (the operating voltage for a continuous electron beam). Consequently, the electron beam current increases rapidly from zero to a stable value (typically 200 μA within 150 ns). The gun is maintained in this ''on'' state for a time sufficient to approach a dynamic equilibrium between excitation and deexcitation processes of the specific target excited states. At time t_1 the potential of L_1 is rapidly changed to a value below the cathode potential, causing blockage of the electron beam. A 200-μA electron beam can be ''turned off'' with this technique with an instrumental time constant of approximately 30 ns. Figure 2(b) shows the expected time dependence of the photon emission rate $I_\lambda(t)$, following pulsed electron impact excitation for both short lifetime ($\tau \ll 30$ ns, dashed

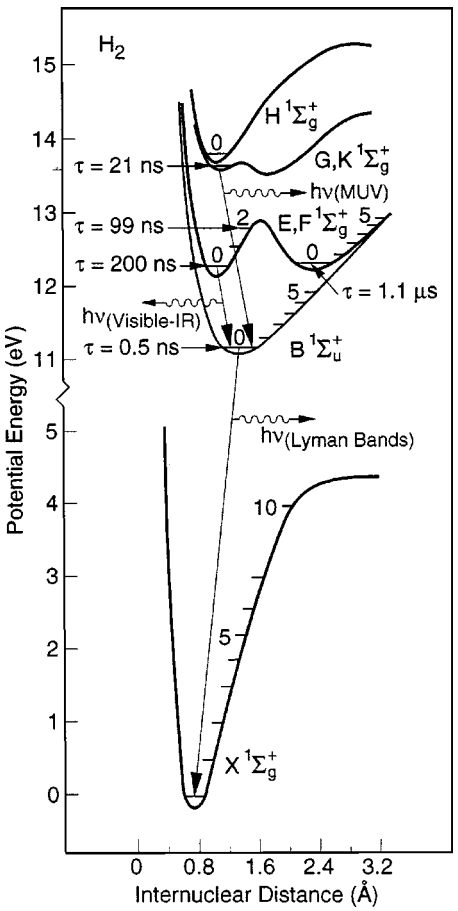

FIG. 1. Potential energy diagram of H_2 for the *B* state and the important double minima cascade states.

line) and relatively long lifetime ($\tau > 30$ ns, solid line) excited states. In general, the time dependence of the photon emission rate is the sum of a decay curve corresponding to radiation from the directly excited resonance state and convolutions of decay curves corresponding to all possible cascade channels with the decay curve of the state populated by cascades. Figure 2(c) depicts the photon gate signal. At time t_2 the rising edge initiates the counting of photons by the data acquisition system. The falling edge at t_3 stops counting shortly before the next pulse period begins. The cross-

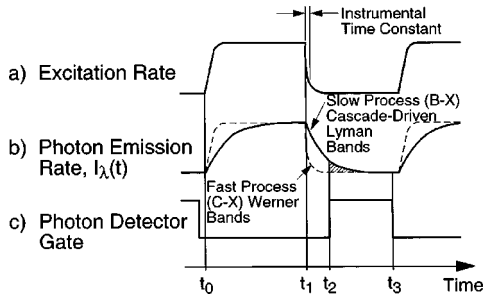

FIG. 2. Pulsed electron gun-timing diagram. (a) Excitation rate of a level in H_2 by the electron beam. (b) Instantaneous intensity from the excited level for fast (dashed) and slow (solid) UV resonance line processes, (c) Photon detector gating.

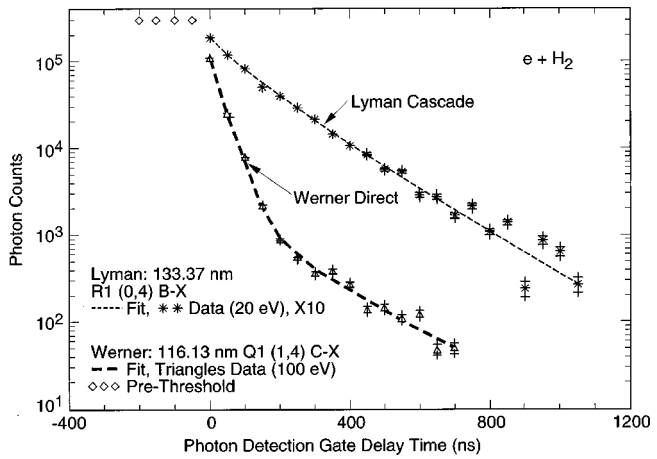

FIG. 3. Variable time photon gate decay curves with respect to gun-off time: (*) Lyman (0,4) band at 133.370 nm and 20 eV electron impact energy and (Δ) Werner (1,4) band at 115.990 nm and 100 eV electron impact energy. Both plots show statistical error bars, with dashed lines representing the respective nonlinear regression fit.

hatched area in Fig. 2(b) schematically represents the number of photons accumulated from t_2 to t_3 and can be represented mathematically as

$$\mathcal{S}_\lambda(t_2) = \int_{t_2}^{t_3} I_\lambda(t)dt, \tag{1}$$

where $\mathcal{S}_\lambda(t_2)$ is the number of photons accumulated from time t_2 to t_3 at wavelength λ and $I_\lambda(t)$ is the time dependence of the photon intensity. The pulsing period as well as ''beam on'' time $(t_1 - t_0)$ and gate delay time $(t_2 - t_1)$ can be varied over a wide range, allowing studies of states characterized by effective lifetimes from tens of nanoseconds to approximately 100 μs. There is a 8-μs long lifetime limit associated with excited H_2 molecules at 300 K escaping from the $1.2° \times 1.9°$ field-of-view of our optical system.

We show in Fig. 3 a variable-gate, pulsed-gun lifetime study of one Lyman (*B*-state) and one Werner (*C*-state) vibrational level of H_2. We use a gun period of 3.5 μs, with a gun-on time of 2.0 μs. The gun-on time of five times the lifetime of the EF state (except the weak $v' = 1$ level of the outer potential well) ensures attainment of asymptotic steady-state conditions for all significant levels of the EF, GK, and H states. Whereas these high-lying states typically cascade to populate the Lyman *B* state, they do not significantly populate any of the Werner levels. For both the gun-on and gun-off part of the cycle, the dashed curve in Fig. 2(b) schematically represents the intensity of the Werner system. The solid curve in Fig. 2(b) represents the cascade-driven Lyman band selected for this study. The photon signal decay curve of the $Q1,R0-R4(1,4)C\text{-}X$ Werner fine structure lines, blended together in a 0.3 nm band-pass (FWHM) centered at 115.99 nm was measured at 100 eV electron impact energy, and is shown in Fig. 3. The lifetime of the rovibronic levels $(v' = 1, J' = 1)$ of the *C* state is 0.9 ns [2] with no low-lying v' Lyman bands present in this band-pass. The photon decay curve of the $R0\text{-}R2(0,4)B\text{-}X$ Lyman fine

structure lines shown in Fig. 3 was measured at 20 eV electron impact energy in a 0.3 nm band pass (FWHM) centered at 133.37 nm. Although the lifetime of the $B(J'=1,v'=0)$ level is 0.5 ns [2], similar to that of the Werner band, the difference between the Lyman and Werner decay curves is striking, indicating the importance of cascade processes. Prompt radiation from the Werner band serves to calibrate the time response of the instrument. The line intensity data shown in Fig. 3, normalized to unity electron beam current and pressure, was evaluated using a nonlinear least-squares curve fit of the form

$$I_\lambda(t)=Q_{\text{fast}}(\lambda)\exp(-t/\tau_{\text{fast}})+Q_{\text{slow}}(\lambda)\exp(-t/\tau_{\text{slow}}), \tag{2}$$

where τ_{fast} and τ_{slow} are the effective lifetimes of the two strongest processes (direct excitation, fast cascade, and/or slow cascade) and $Q_{\text{fast}}(\lambda)$ and $Q_{\text{slow}}(\lambda)$ are the emission cross sections of these processes. It should be noted that τ_{fast} and τ_{slow} do not represent the lifetimes of individual states, rather the combined effect of several transitions with similar lifetimes. The measured lifetime value of $\tau_{\text{fast}}=30$ ns in Fig. 3 for the C-X decay is a measure of the instrumental time constant. The Werner C-X transition shown in Fig. 3 has a weak secondary process with a lifetime of 140 ± 50 ns, with $Q_{\text{fast}}/Q_{\text{slow}}>40$. We attribute this to the cumulative effects of weak cascade processes from Rydberg gerade states GK-C, H-C, J-C as reported by Huber and Herzberg in Ref. [12]. This parameter was also verified by monitoring the time decay of the Faraday cup current during the gun-off part of the pulsing cycle. The present experiment cannot distinguish direct excitation and cascade processes that have lifetimes less than 40 ns. It was not the goal of this program to measure the prompt lifetimes of the direct excitation transition but rather to study the slow cascade late in the decay curve.

The Lyman band is analyzed in the same manner. Based on a comparison of direct excitation and cascade Franck-Condon factors [13,1], the $v'=0$ level is found to be populated mostly by cascade at 20 eV electron impact energy, with less than 10% direct excitation. The effective experimental lifetimes were found to be 51 ns for the fast cascade processes (τ_{fast}), and 161 ns for the slow cascade processes (τ_{slow}). The ratio of the cross sections $Q_{\text{fast}}/Q_{\text{slow}}<1$ indicates that the slow cascade cross section is larger. The Lyman band decay curve time constants are a weighted average of lifetimes from rovibronic transitions of the $n=2$ EF and $n=3$ GK, H states. The strongly excited EF vibrational levels of the inner potential well, $v'=0,1,2,3$, have lifetimes from 99 to 203 ns whereas the strongly excited GK, H levels, $v'=0,1,2$ have lifetimes of 20–100 ns [10,9]. The $n=4$ I and J states with lifetimes of 10–20 ns for $v'=0$ are probably not observed, since the excitation cross sections of these states are expected to be small. We, therefore, interpret the stronger, slow component of the decay curve as arising mainly from transitions from the EF double-minimum state (where the lower vibrational levels of the E-state inner potential well favor decay to the $B\,v'=0$ level) and the weaker, faster decay curve as arising mainly from transitions involving the GK, H double-minimum states.

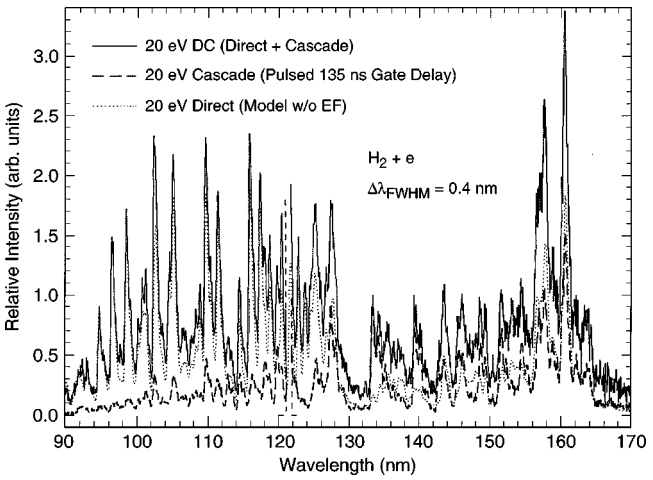

FIG. 4. 20 eV (0.4 nm FWHM) steady-state (cascade+direct) spectrum (solid line) with the regression fit components to the spectrum: (1) The dashed line represents the 20 eV pulsed-gun cascade spectrum, (2) the dotted line gives the 20 eV model direct excitation spectrum, and (3) the short dashed line shows H Ly-α.

The experimental decay curves, shown in Fig. 3, establish the gate delay time needed to observe a cascade spectrum, free of any directly excited Rydberg bands. At a gate delay time of $t_2-t_1=135$ ns after the electron beam blockage has occurred, the Werner band intensity has decreased by a factor 40, while the $v'=0$ Lyman band is down by only a factor 3. For a gate delay time of 135 ns we show in Fig. 4 the cascade spectrum of the Lyman bands (0.4 nm FWHM). The spectrum was obtained by accumulating photon counts from $t_2-t_1=135$ ns (Fig. 2) to $t_3-t_1=1400$ ns for each wavelength. The UV spectrum from 90–170 nm is calibrated by techniques previously published [14,1]. The low-resolution wavelength structure in Fig. 4 is indicative of strong B-$X\,v'=0,1,2$-v'' progressions. However, high vibrational levels ($v'=19$) of the B state must be weakly excited by cascade in order to explain the full spectrum to the ~92 nm short wavelength threshold for this progression. The cascade spectrum is compared to the steady-state electron beam spectrum (cascade+direct) and the Rydberg band system direct spectrum, which we have recently modeled, including a complete set of 100 eV absolute cross sections for the B,C,D,B' states, $n=2,3$ [14]. The regression analysis of the steady-state spectrum in Fig. 4 establishes the cascade cross section. The channel (0.05 nm/channel) intensities of the experimental cascade spectrum and the direct excitation model spectrum are used mathematically as independent vectors in the regression analysis. The regression analysis determines a linear combination of these vectors that are summed to fit the steady state spectrum. The rms best fit comparison between regression model and data for the wavelength interval 90–170 nm for the 1600 data points is 98% with the major discrepancies occurring at the unmodeled Lyman H lines from dissociative excitation for $n>2$ (e.g., H Ly-β at 102.6 nm).

The component fits to the steady-state spectrum are

shown in Fig. 4. The regression model (not shown) is itself indistinguishable from the experimental steady state spectrum. Liu *et al.* [15] give the direct excitation cross section of the Lyman bands at 20 eV as $2.0\times10^{-17}\,\mathrm{cm}^2$. Based on the 100 eV Rydberg cross sections of Jonin *et al.* [14] and the excitation function of Liu *et al.*, the cross section for the Rydberg bands (including the Lyman bands) at 20 eV is established as $3.90\times10^{-17}\,\mathrm{cm}^2$. The cascade cross section is proportional to the area under the cascade spectrum (dashed curve, Fig. 4). The B-X cascade cross section was measured to be $1.7\pm0.5\times10^{-17}\,\mathrm{cm}^2$ at 20 eV with less than 10% C-X cascade and $H_2(a\text{-}b)$ continuum cascade in the cross section measurement.

The spectral patterns from direct excitation and cascade are different. Direct excitation produces a large population in the B state centered at $v'=7$, whereas cascade populates the lower vibrational levels most strongly, beginning at $v'=0$. This can be seen in Fig. 4 which shows that there are distinct regions in the spectrum dominated by either direct or cascade processes. The region below 130 nm is dominated by direct excitation processes, whereas the most important two wavelength regions that are exclusively (more than 90%) due to cascade lie near 133–135 nm and 139–142 nm. These regions correspond to the rotational lines of the (0, 4) and (0, 5) vibrational bands of the B-X Lyman system, the two strongest bands of the $v'=0$, the strongest v'' progression. Detailed rotational line identifications are given in the H_2 spectral atlas of Roncin and Launay [16]. Recently, James, Ajello, and Pryor [17] reported the 19 eV emission cross sections of the GK,H,I,J$\cdots\rightarrow$B cascade bands in the middle ultraviolet from 200–500 nm to be about $1.3\times10^{-18}\,\mathrm{cm}^2$. This value represents a lower limit, since an additional 10–20 % of these band systems lie longward of 500 nm. Therefore, we estimate from this study that the EF state must produce about 80–90 % of the intensity of the cascading band systems.

Additional regression analysis of a pulsed spectrum and steady state spectrum pair measured at 100 eV showed the cascade cross section to be $5.0\pm0.6\times10^{-18}\,\mathrm{cm}^2$. The 100 eV cross section for the B-X cascade is 70% larger than the previous value of $2.9\times10^{-18}\,\mathrm{cm}^2$ recommended by Ajello *et al.* [18]. The change in relative cross section from 20 to 100 eV, a factor of 3.4, is matched by earlier estimates [19]. However, the earlier absolute cross sections were based on an inaccurate spectral model, which underestimated the spectral content (and hence the cross section) by 70% and further validates the experimental method of this paper.

In conclusion, a method has been established for measuring electron-excited cascade spectra of the UV resonance structure of atoms and molecules, which have strong cascade contributions. A significant cascade contribution can drastically change the emerging UV spectrum from the known direct excitation spectrum. In addition, we can use this method to measure the energy dependence of cascade cross sections and effective cascade lifetimes for resonance transitions in the UV.

The research described in this paper was carried out at the Jet Propulsion Laboratory, California Institute of Technology, and was sponsored by the Air Force Office of Scientific Research, the Aeronomy Program of the National Science Foundation (ATM-9320589) and NASA Planetary Atmospheres and Space Astrophysics Research branches. D. D. and D. L. H. are supported by the National Research Council.

[1] X. Liu *et al.*, Astrophys. J. **101**, 375 (1995).
[2] H. Abgrall *et al.*, Astron. Astrophys. (to be published).
[3] J. M. Ajello *et al.*, J. Geophys. Res. **103**, 20125 (1998).
[4] A. L. Broadfoot *et al.*, Science **246**, 1459 (1989).
[5] J. C. Raymond, W. P. Blair, and K. S. Long, Astrophys. J. **489**, 314 (1997).
[6] H. Abgrall, *et al.*, Can. J. Phys. **72**, 856 (1994).
[7] A. H. Mahan, A. Gallagher, and S. J. Smith, Phys. Rev. A **13**, 156 (1976).
[8] L. Wolniewicz and K. J. Dressler, J. Chem. Phys. **100**, 444 (1994).
[9] D. W. Chandler and L. Thorne, J. Chem. Phys. **85**, 1733 (1986).
[10] M. Glass-Maujean *et al.*, J. Chem. Phys. **80**, 4355 (1984).
[11] K. Tsukiyama, J. Ishii, and T. Kasuya, J. Chem. Phys. **97**, 875 (1992).
[12] K. P. Huber and G. Herzberg, *Molecular Spectra and Molecular Structure: IV, Constants of Diatomic Molecule* (Van Nostrand, New York, 1979), p. 250.
[13] R. J. Spindler, J. Quant. Spectrosc. Radiat. Transf. **9**, 1041 (1969).
[14] C. Jonin *et al.*, Appl. J. Suppl. (to be published).
[15] X. Liu *et al.*, J. Geophys. Res. **103**, 26739 (1998).
[16] J.-Y. Roncin and F. Launay, *Atlas of the Vacuum Ultraviolet Emission Spectrum of Molecular Hydrogen* [J. Phys. Chem. Ref. Data Monogr. No. 4, (AIP, Woodbury, NY, 1994)].
[17] G. K. James, J. M. Ajello, and W. Pryor, J. Geophys. Res. **103**, 20113 (1998).
[18] J. M. Ajello *et al.*, Appl. Opt. **27**, 890 (1988).
[19] D. E. Shemansky, J. M. Ajello, and D. T. Hall, Astrophys. J. **296**, 765 (1985).